

Introducing an Electrochemical Impedance Spectroscopy Methodology based on Volterra Filters

Simone Orcioni,^{*} Alberto Carini[†], Alessandro Mauri[†], Chiara Giosuè[‡], Daniele Marchese[◊], Massimo Conti^{*}

^{*}Department of Information Engineering, Università Politecnica delle Marche, Ancona, Italy.

[†]Department of Engineering and Architecture, University of Trieste, Trieste, Italy.

[‡]Department of Materials, Environmental Sciences and Urban Planning, Università Politecnica delle Marche, Ancona, Italy.

[◊]MIDAC Spa, 37038 Soave, Italy.

Abstract—The paper proposes a novel Electrochemical Impedance Spectroscopy methodology that takes into account the nonlinearities present in the battery. For this purpose, the current-voltage relationship of the cell is modeled in discrete domain as a Volterra filter and the linear part of the nonlinear model is efficiently estimated using Orthogonal Periodic Sequences. Preliminary experimental results involving six lithium-ion cells show the soundness of the proposed approach also in comparison with the classical method.

Index Terms—Electrochemical Impedance Spectroscopy, Volterra series, Lithium-ion batteries.

I. INTRODUCTION

The demand for lithium-ion batteries (LIBs) has been rising in recent years, mainly to fulfil by 2050 the Green Deal aims [1] going through the carbon-neutral mobility milestone by 2035 [2]. Currently, LIBs are the main technology capable of delivering high energy density and peak power performance while offering a good compromise between size and cost. Nonetheless, what should be avoided is shifting the problem from greenhouse emissions to supplying raw materials as well as having disposal issues. The circular economy may drive the transition via its principles of reducing, reusing, and recycling. The aim of the present work is to be consistent with the principle of reusing, conforming to the second life approach for LIBs [1], [2].

The reasons for battery aging can basically be subdivided into three groups, which are the loss of active materials, the loss of cyclable lithium, and the deterioration of ionic kinetics [3]. In general, the consequences of aging in lithium-ion cells are the loss of capacity and the reduction of power capability due to increased impedance. This interaction between capacity fade and impedance increase caused by the formation, thickening, and reconstruction of anode and cathode layers has been investigated in the literature, see for example [4].

A widespread non-invasive offline method to investigate this behavior is the Electrochemical Impedance Spectroscopy (EIS). This is a perturbative characterization of the dynamic of an electrochemical process used to unravel complex nonlinear processes. The study of the impedance of a LIB provides hidden information about the electrochemical condition within the cell and it is useful for the evaluation of its state. It has been widely used to describe different LIB aspects like aging phenomena [5], developing of Battery Management

System (BMS) [6], State of Charge (SoC) and State of Health (SoH) estimation [7], [8], equivalent parameters evaluation and modeling [9]–[13]. In spite of the different purposes, the EIS method is often performed with a stimulation of the battery via tones [14].

The aim of the present work is to propound a new way to estimate the LIB impedance for EIS purposes, introducing a nonlinear model of the LIB by means of Volterra filters. These filters derive directly from the truncation in order and memory of the Volterra series [15], a polynomial functional series widely used for nonlinear system representation and identification [16], [17]. Once established with the Stone-Weierstrass theorem that any discrete-time, causal, time-invariant, continuous system can be arbitrarily well approximated with a Volterra filter [18], the problem of approximating its parameters can be faced with conventional methods, based on cross-correlation with stochastic inputs [19]–[22], or with those using deterministic inputs like perfect periodic sequences [18], [23], or more recently Orthogonal Periodic Sequence (OPS) [24]. The peculiarity of this technique is that, through the identification of the Volterra series, we obtain the output as the sum of polynomial functionals of increasing order. By taking only the filter coefficients of the first order part we obtain, net of identification errors, the true linear relationship between input and output. This is what is usually approximated with the small signal analysis of the nonlinear system.

The rest of the paper is organized as follows. Section II reviews the Volterra filters. Section III discusses the proposed method and the identification techniques adopted. Section IV presents the experimental results and Section V concludes the paper.

II. THE DISCRETE-TIME VOLTERRA FILTERS

Volterra filters are polynomial linear-in-the-parameters (LIP) nonlinear filters, i.e., their output depends linearly on the coefficients, and they are universal approximators, i.e., they can arbitrarily well approximate any discrete-time, time-invariant, finite memory, continuous nonlinear system,

$$y(n) = f[x(n), x(n-1), \dots, x(n-M+1)] \quad (1)$$

where f is a continuous function from \mathbb{R}^M to \mathbb{R} , x is the system input, with $x(n) \in [-1, +1]$, and M is the length of its memory.

A Volterra filter of order P , diagonal number D , memory M has the input-output relationship in diagonal form given by

$$\begin{aligned}
y(n) = & h_0 + \sum_{j=0}^{M-1} h_1(j)x(n-j) \\
& + \sum_{i_1=0}^D \sum_{j=0}^{M-1-i_1} h_2(i_1, j)x(n-j)x(n-j-i_1) \\
& + \dots + \sum_{i_1=0}^D \sum_{i_2=i_1}^D \dots \sum_{i_{P-1}=i_{P-2}}^D \sum_{j=0}^{M-1-i_{P-1}} h_P(i_1, \dots, i_{P-1}, j) \\
& x(n-j)x(n-i_1-j) \dots x(n-j-i_{P-1}). \quad (2)
\end{aligned}$$

Using the terminology of Volterra filters, it is composed of a constant term h_0 , a first-order (or linear) kernel $h_1(i)$, the second-order kernel $h_2(i_1, j)$, and higher p -th order kernels $h_p(\cdot)$, with $p \leq P$.

The diagonal number D is the maximum time difference between the samples involved in the products. Since real nonlinear systems tend to concentrate most of the energy on the terms with low diagonal numbers [18], in nonlinear system identification it is often convenient to limit D to low values.

III. THE PROPOSED METHOD

The LIB can be considered a nonlinear system and the EIS aims to estimate the linear part of the system relation between voltage and current. By modeling the LIB with the Volterra filter representation given in (2), the EIS problem reduces to the estimation of the coefficients $h_1(j)$ of the Volterra filter, for $j = 0, \dots, M-1$. To contrast the effect of nonlinearities, the linear part is usually estimated using small amplitude sinusoids to guarantee that all polynomial terms of order greater than 1 in (2) can be neglected. In this paper, we follow a different approach and we consider an identification method that is a priori robust towards the nonlinearities. The coefficients $h_1(j)$ are efficiently identified using an OPS [24], [25] and the cross-correlation method, i.e., computing the cross-correlation between the output signal and an appropriate OPS. The OPS identifies the desired coefficients $h_1(j)$ very efficiently since the cross-correlation can be computed using the Fast Fourier Transform (FFT), but it could amplify the effect of noise on the output signal, as explained in [24], [25]. To ascertain the goodness of the result, we have performed the same identification also with the classical least-square (LS) approach. In this section, we review the OPSs and LS approaches applied to Volterra filters.

A. Orthogonal Periodic Sequences

Let us consider the Volterra filter in (2) and assume to apply as input a persistently exciting periodic signal of period L . The input is persistently exciting when its samples are randomly taken from a Gaussian distribution, a white uniform distribution, or another random distribution. The samples can also be quantized, provided a sufficiently large number of quantization levels is used.

By definition, an OPS is a periodic sequence of period L that cross-correlated with the filter output provides one of the so-called ‘‘diagonals’’ of the filter [24]. One of the diagonals is the set of coefficients $h_1(j)$ for $0 \leq j \leq M-1$.

While all the coefficients of the Volterra filter could be estimated using appropriate OPSs [24], in EIS we are interested only in the identification of the linear diagonal $h_1(j)$, and the OPS sequence $z_1(n)$ is built so that

$$h_1(j) = \langle y(n)z_1(n-j) \rangle_L \quad (3)$$

for $0 \leq j \leq M-1$ and with $\langle \cdot \rangle_L$ indicating the sum of the terms between brackets over a period L . By replacing (2) in (3), it can be proved that (3) is satisfied if $\langle x(n)z_1(n) \rangle_L = 1$ and if $z_1(n)$ is orthogonal to all other products of x in (2), e.g., $\langle x(n-j)x(n-i_1-j) \dots x(n-j-i_{P-1})z_1(n) \rangle_L = 0$. By imposing these conditions, for sufficiently large L an under-determined linear system having as variables the samples of $z_1(n)$ for $n \in [0, M-1]$ is obtained. Solving this linear system, an OPS can be developed for any Volterra filter of order P , diagonal number D , memory M , and for the chosen periodic input sequence. Once available $z_1(n)$, the coefficients $h_1(j)$ can be estimated from (3), which requires one period of the measured output sequence $\hat{y}(n)$. To extract a period of $\hat{y}(n)$, the input sequence has to be applied sufficiently long to guarantee stationary conditions over a period, thus at least for $L+M$ samples if the nonlinear system has memory M .

It was shown in [24] that the cross-correlation with the OPS can amplify the effect of noise with respect to the LS identification unless a sufficiently large period L is considered. To verify that the noise does not affect the measurement, we have also identified the battery with the classical LS method using the same OPS input and output sequences.

B. Least-Square Method

To identify the linear part of the Volterra filter in (2) with the LS method all its coefficients have to be estimated. The input-output relationship in (2) can also be written in vector form as

$$y(n) = \mathbf{h}^T \mathbf{x}(n) \quad (4)$$

where \mathbf{h} is the vector collecting all the coefficients, $\mathbf{h} = [h_0, h_1(0), \dots, h_1(M-1), h_2(0,0), \dots]^T$, and $\mathbf{x}(n)$ the vector collecting the corresponding monomials, $\mathbf{x}(n) = [1, x(n), \dots, x(n-M+1), x^2(n), \dots]^T$. The LS method finds the coefficient vector \mathbf{h} that minimizes $\langle e^2(n) \rangle_L$, with $e(n) = \hat{y}(n) - \mathbf{h}^T \mathbf{x}(n)$ and $\hat{y}(n)$ the measured output. It can be proved that

$$\mathbf{h} = [\langle \mathbf{x}(n)\mathbf{x}^T(n) \rangle_L]^{-1} \langle \mathbf{x}(n)\hat{y}(n) \rangle_L. \quad (5)$$

It should be noticed that while the OPS method has a computational cost of $2L \log_2 L$ multiplications working in the FFT domain, the LS method in (5) has a computational cost of $R^2 L$ multiplication, where R is the number of coefficients of the Volterra filter which is usually much larger than $\log_2 L$. The larger computational cost is acceptable for the comparison performed in this paper, but it would be unacceptably large for an instrument with limited computational power.



Fig. 1: Experimental setup.

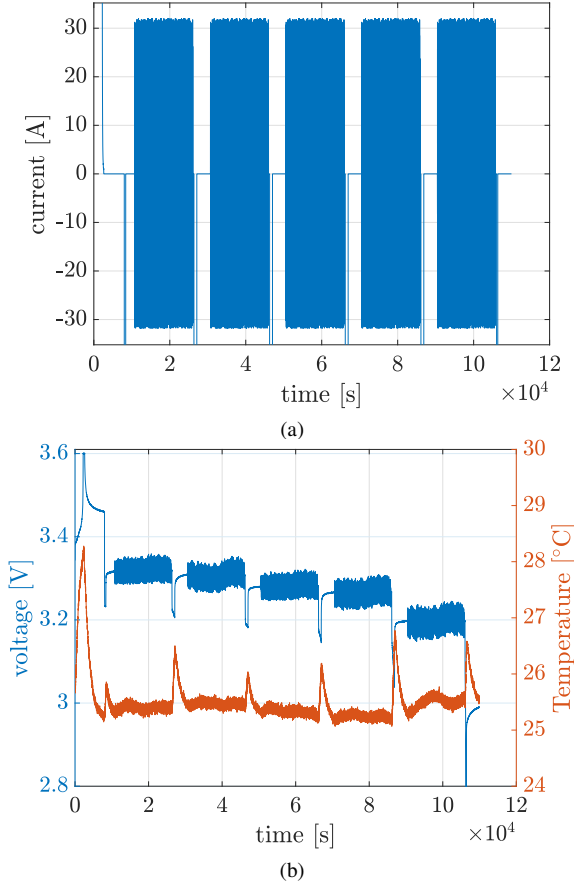


Fig. 2: (a) Input current for the EIS estimation at different SoC levels. (b) Corresponding voltage of Cell #1.

In the experimental results, the identifications of $h_1(n)$ with (3) and (5) will be compared in terms of Normalized Root Mean Square Deviation (NRMSD), which is defined as follows

$$\text{NRMSD} = \sqrt{\frac{(\mathbf{h}_{1\text{OPS}} - \mathbf{h}_{1\text{LS}})^T (\mathbf{h}_{1\text{OPS}} - \mathbf{h}_{1\text{LS}})}{\mathbf{h}_{1\text{OPS}}^T \mathbf{h}_{1\text{OPS}}} \quad (6)$$

where $\mathbf{h}_{1\text{OPS}}$ is the coefficient vector estimated with (3) and $\mathbf{h}_{1\text{LS}}$ the corresponding coefficient vector obtained from (5).

IV. EXPERIMENTAL RESULTS

The experimental set up has been applied to six commercial lithium iron phosphate (LiFePO₄/LFP) cells cycled from 100% to 80% of the nominal capacity: four have 60 Ah

of nominal capacity while the remaining have 50 Ah. All have nominal voltage equal to 3.2 V, dimensions equal to 37 mm × 101 mm × 192 mm, internal resistance ≤ 2 m Ω , a discharge voltage limit of 2.5 V, a charge voltage limit of 3.8 V, 1C rate as the maximum discharge rate, and a weight < 1400 g. With 1C current, i.e., one capacity current in battery terminology, the battery charges or discharges in one hour.

The EIS estimation was performed during an aging campaign performed with the regenerative battery pack test system Chroma Model 17020E. The cells have been cycled in a climatic chamber to maintain the temperature at 25 °C. Fig. 1 shows the experimental setup.

The characterization procedure consists of a complete charging step at constant current (CC) and constant voltage (CV) followed by CC discharge and OPS applications steps. The aging consists in a sequence of about 5000 charge/discharge cycles from 100% to 80% of the nominal capacity. The characterization steps, in details, are:

- 1) CC charge 1C up to 3.6 V & CV charge until the current reaches 500 mA (about 1 h) & Rest for 600 s
- 2) CC discharge at 1C for 10% of ΔSoC & Rest for 300 s
- 3) OPS (16960 pulses with $T_s = 0.9$ s and $\text{ampl.} = 32$ A)
- 4) CC discharge at 1C for 20% of ΔSoC
- 5) Rest for 600 s
- 6) Steps 3-5 repeated for SoC = 90%, 70%...10%

The aging steps are:

- 1) CC charge at 1C up to 3.6 V (about 1 h) & CV charge until the current reaches 500 mA (about 600 s) & Rest for 5400 s
- 2) CC discharge at 1C (about 1 h) & Rest for 5400 s
- 3) Loop back to step 1 for 500 times (approximate SoH reduction of 2%).

Fig. 2 shows the current applied to the test Cell #1, the measurements of voltage and temperature performed by the Chroma 17020E during the characterization steps. The SoC reduction to 90%, 70%, 50%, 30% 10% is evidenced during the measurements by the reduction of the open circuit voltage.

Biologic HCP-1005 potentiostat was used as a reference for the EIS. The measurement steps performed by the Biologic HCP-1005 are similar to the characterization cycle performed with Chroma 17020E, but the built-in EIS estimation was used for each of the chosen SoC. The EIS estimation was performed for 30 frequency points in the range from 10 kHz to 10 mHz.

Fig. 3 reports the Nyquist plot obtained by using the proposed methodology (the continuous lines) with an OPS for a Volterra filter of order $P = 2$, diagonal number $D = 0$, memory length $M = 128$. The OPS parameters P , D , and M were selected with a trial and error procedure using the same input-output signals. In Fig. 3, $\Re(Z(f))$ and $\Im(Z(f))$ are the real and imaginary parts of the impedance at frequency f , estimated with the FFT of the measured linear kernel h_1 . The proposed methodology was applied to three almost new cells (SoH 98%). For comparison, the lines with markers report the results obtained by using built-in Biologic HCP-1005 technique in the same conditions. The Figure displays

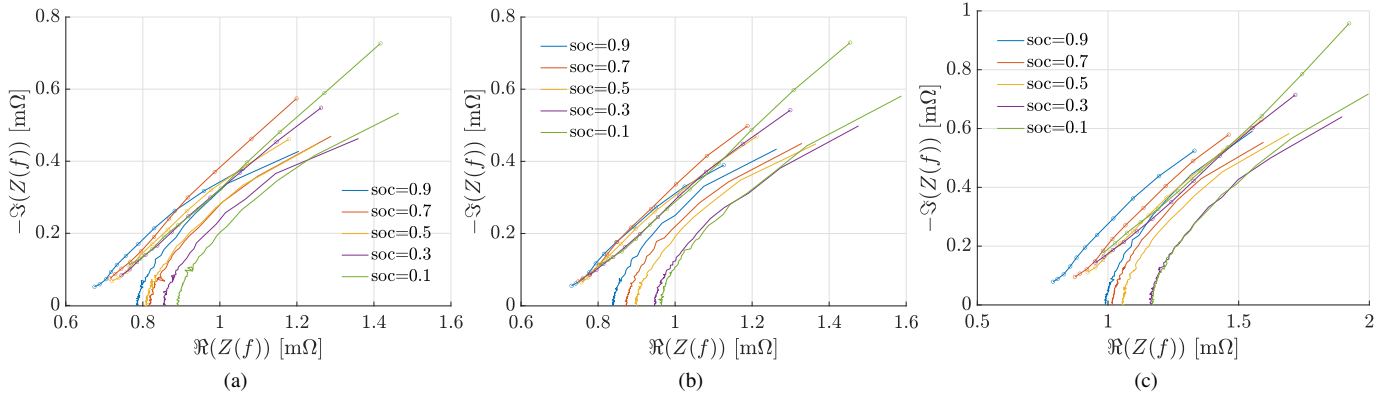


Fig. 3: Comparison of Nyquist plot results obtained with the methodology proposed (solid lines) against those obtained with Biologic HCP-1005 (lines with markers). The cells are aged at 98% of nominal capacity: (a) cell #1 $C_{\text{nom}} = 60$ Ah; (b) cell #3 $C_{\text{nom}} = 60$ Ah; (c) cell #5 $C_{\text{nom}} = 50$ Ah.

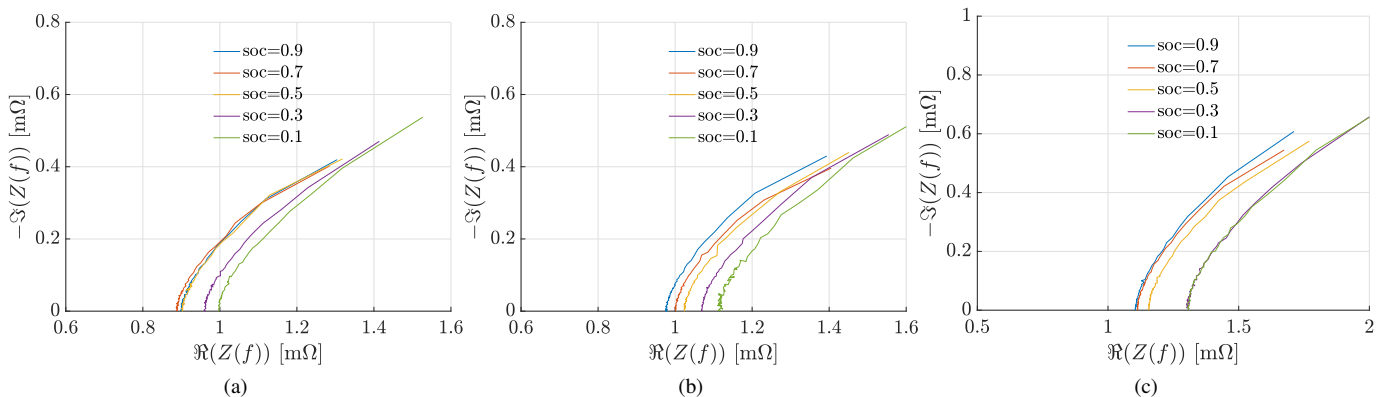


Fig. 4: Nyquist plot of aged cells at 88% of nominal capacity; (a) cell #1; (b) cell #3; (c) cell #5.

TABLE I: NRMSD averaged over different SoC levels for each cell, order $P = 2$, $D = 0$, $M = 128$.

Cell #1	Cell #2	Cell #3	Cell #4	Cell #5	Cell #6
$2.25 \cdot 10^{-3}$	$2.39 \cdot 10^{-3}$	$2.21 \cdot 10^{-3}$	$2.15 \cdot 10^{-3}$	$2.32 \cdot 10^{-3}$	$2.62 \cdot 10^{-3}$

results in a range of frequencies that goes from $f_{\min} = \frac{F_s/2}{M}$ to $F_s/2$, where F_s is the sampling frequency $F_s = \frac{1}{0.9}$ Hz.

The obtained results by the two methodologies are similar. The real part of the results obtained with the Volterra filter is lightly higher (about 0.1 mΩ with respect to the reference). The real part of the impedance increases while SoC decreases. This result is in agreement with the other models reported in the literature (for example [26]) that shows an increasing value of the series resistance while SoC decreasing. Fig. 4 reports the Nyquist plot, obtained using the proposed methodology, applied to three cells, #1, #3, and #5 after 3000 charge-discharge cycles (SoH about 88%). A light right shift of the curves can be observed in comparison with the results of the same cells before aging shown in Fig. 3.

Table I provides the NRMSD between the coefficients obtained with the proposed method and the LS approach. For each cell, the NRMSD was averaged over five measurements at the different SoC (90%, 70%, 50%, 30%, 10%). The average

between the different cells is equal to $2.3 \cdot 10^{-3}$, which is a very small value.

V. CONCLUSION

The proposed methodology has been applied to the characterization of six lithium-ion batteries during the aging process. The results are successfully compared with the classical impedance measurement method based on small signals analysis. This constraint implies the use of accurate and high cost measurement instruments. One of the advantages of the proposed methodology is that the linear response of the battery can be obtained also applying large signals to identify the system and considering only the Volterra filter coefficients that make up the linear part. Therefore instruments like source-measurement units with lower resolution can be used for the identification. This aspect opens the possibility of the battery impedance measurement and SoH estimation also in real time during daily battery life using the BMS itself.

REFERENCES

- [1] C. Giosuè, D. Marchese, M. Cavalletti, R. Isidori, M. Conti, S. Orcioni, M. L. Ruello, and P. Stipa, "An exploratory study of the policies and legislative perspectives on the end-of-life of lithium-ion batteries from the perspective of producer obligation," *Sustainability*, vol. 13, no. 20, p. 11154, oct 2021.
- [2] European Technology and Innovation Platform on Batteries. (2020, 04) Batteries Europe. https://ec.europa.eu/energy/system/files/documents/batteries_europe_strategic_research_agenda_december_2020__1.pdf.
- [3] S. Grolleau, A. Delaille, H. Gualous, P. Gyan, R. Revel, J. Bernard, E. Redondo-Iglesias, and J. Peter, "Calendar aging of commercial graphite/LiFePO₄ cell - predicting capacity fade under time dependent storage conditions," *Journal of Power Sources*, vol. 255, pp. 450–458, 2014.
- [4] S. F. Schuster, M. J. Brand, C. Campestrini, M. Gleissenberger, and A. Jossen, "Correlation between capacity and impedance of lithium-ion cells during calendar and cycle life," *Journal of Power Sources*, vol. 305, pp. 191–199, 2016.
- [5] P. Iurilli, C. Brivio, and V. Wood, "On the use of electrochemical impedance spectroscopy to characterize and model the aging phenomena of lithium-ion batteries: a critical review," *Journal of Power Sources*, vol. 505, p. 229860, sep 2021.
- [6] E. Din, C. Schaef, K. Moffat, and J. T. Stauth, "A scalable active battery management system with embedded real-time electrochemical impedance spectroscopy," *IEEE Transactions on Power Electronics*, vol. 32, no. 7, pp. 5688–5698, jul 2017.
- [7] M. Messing, T. Shoa, and S. Habibi, "Estimating battery state of health using electrochemical impedance spectroscopy and the relaxation effect," *Journal of Energy Storage*, vol. 43, p. 103210, nov 2021.
- [8] Q. Zhang, C.-G. Huang, H. Li, G. Feng, and W. Peng, "Electrochemical impedance spectroscopy based state of health estimation for lithium-ion battery considering temperature and state of charge effect," *IEEE Transactions on Transportation Electrification*, pp. 1–1, 2022.
- [9] P. Vyroubal and T. Kazda, "Equivalent circuit model parameters extraction for lithium ion batteries using electrochemical impedance spectroscopy," *Journal of Energy Storage*, vol. 15, pp. 23–31, feb 2018.
- [10] M. Kasper, A. Leike, J. Thielmann, C. Winkler, N. Al-Zubaidi R-Smith, and F. Kienberger, "Electrochemical impedance spectroscopy error analysis and round robin on dummy cells and lithium-ion-batteries," *Journal of Power Sources*, vol. 536, p. 231407, jul 2022.
- [11] D. Andre, M. Meiler, K. Steiner, C. Wimmer, T. Soczka-Guth, and D. Sauer, "Characterization of high-power lithium-ion batteries by electrochemical impedance spectroscopy. I. experimental investigation," *Journal of Power Sources*, vol. 196, no. 12, pp. 5334–5341, jun 2011.
- [12] D. Andre, M. Meiler, K. Steiner, H. Walz, T. Soczka-Guth, and D. Sauer, "Characterization of high-power lithium-ion batteries by electrochemical impedance spectroscopy. II: Modelling," *Journal of Power Sources*, vol. 196, no. 12, pp. 5349–5356, jun 2011.
- [13] I. Ezpeleta, L. Freire, C. Mateo-Mateo, X. R. Nóvoa, A. Pintos, and S. Valverde-Pérez, "Characterisation of commercial Li-Ion batteries using electrochemical impedance spectroscopy," *ChemistrySelect*, vol. 7, no. 10, mar 2022.
- [14] M. Koseoglou, E. Tsioumas, D. Papagiannis, N. Jabbour, and C. Mademlis, "A novel on-board electrochemical impedance spectroscopy system for real-time battery impedance estimation," *IEEE Transactions on Power Electronics*, vol. 36, no. 9, pp. 10776–10787, sep 2021.
- [15] V. J. Mathews and G. L. Sicuranza, *Polynomial Signal Processing*. New York, NY: Wiley, 2000.
- [16] V. Z. Marmarelis, *Nonlinear Dynamic Modeling of Physiological Systems*. Wiley-IEEE Press, 2004.
- [17] S. Orcioni, A. Terenzi, S. Cecchi, F. Piazza, and A. Carini, "Identification of volterra models of tube audio devices using multiple-variance method," *Journal of the Audio Engineering Society*, vol. 66, no. 10, pp. 823–838, oct 2018.
- [18] A. Carini, S. Cecchi, and S. Orcioni, "Orthogonal LIP nonlinear filters," in *Adapt. Learn. Methods Nonlinear Syst. Model.*, D. Comminello and J. C. Principe, Eds. Elsevier, 2018, ch. 2, pp. 15–46.
- [19] Y. W. Lee and M. Schetzen, "Measurement of the Wiener kernels of a non-linear system by cross-correlation," *International Journal of Control*, vol. 2, no. 3, pp. 237–254, 1965.
- [20] M. Pirani, S. Orcioni, and C. Turchetti, "Diagonal kernel point estimation of nth-order discrete volterra-wiener systems," *EURASIP Journal on Advances in Signal Processing*, vol. 2004, no. 12, pp. 1807–1816, sep 2004.
- [21] S. Orcioni, M. Pirani, and C. Turchetti, "Advances in Lee-Schetzen method for Volterra filter identification," *Multidimensional Systems and Signal Processing*, vol. 16, no. 3, pp. 265–284, 2005.
- [22] S. Orcioni, "Improving the approximation ability of Volterra series identified with a cross-correlation method," *Nonlinear Dynamics*, vol. 78, no. 4, pp. 2861–2869, dec 2014.
- [23] A. Carini, S. Cecchi, and S. Orcioni, "Robust room impulse response measurement using perfect periodic sequences for Wiener nonlinear filters," *Electronics*, vol. 9, no. 11, p. 1793, oct 2020.
- [24] A. Carini, S. Orcioni, A. Terenzi, and S. Cecchi, "Orthogonal periodic sequences for the identification of functional link polynomial filters," *IEEE Transactions on Signal Processing*, vol. 68, pp. 5308 – 5321, may 2020.
- [25] A. Carini, S. Cecchi, A. Terenzi, and S. Orcioni, "A room impulse response measurement method robust towards nonlinearities based on orthogonal periodic sequences," *IEEE/ACM Transactions on Audio, Speech, and Language Processing*, vol. 29, pp. 3104–3117, 2021.
- [26] S. Orcioni, L. Buccolini, A. Ricci, and M. Conti, "Lithium-ion battery electrothermal model, parameter estimation, and simulation environment," *Energies*, vol. 3, no. 10, pp. 1–20, 2017.